

Research Article

Methodology for Assessing the Probability of Corrosion in Concrete Structures on the Basis of Half-Cell Potential and Concrete Resistivity Measurements

Lukasz Sadowski

Institute of Building Engineering, Wrocław University of Technology, Plac Grunwaldzki 11, 50-377 Wrocław, Poland

Correspondence should be addressed to Lukasz Sadowski; lukasz.sadowski@pwr.wroc.pl

Received 27 March 2013; Accepted 29 April 2013

Academic Editors: S. Chen and Q. Q. Liang

Copyright © 2013 Lukasz Sadowski. This is an open access article distributed under the Creative Commons Attribution License, which permits unrestricted use, distribution, and reproduction in any medium, provided the original work is properly cited.

In recent years, the corrosion of steel reinforcement has become a major problem in the construction industry. Therefore, much attention has been given to developing methods of predicting the service life of reinforced concrete structures. The progress of corrosion cannot be visually assessed until a crack or a delamination appears. The corrosion process can be tracked using several electrochemical techniques. Most commonly the half-cell potential measurement technique is used for this purpose. However, it is generally accepted that it should be supplemented with other techniques. Hence, a methodology for assessing the probability of corrosion in concrete slabs by means of a combination of two methods, that is, the half-cell potential method and the concrete resistivity method, is proposed. An assessment of the probability of corrosion in reinforced concrete structures carried out using the proposed methodology is presented. 200 mm thick 750 mm × 750 mm reinforced concrete slab specimens were investigated. Potential E_{corr} and concrete resistivity ρ in each point of the applied grid were measured. The experimental results indicate that the proposed methodology can be successfully used to assess the probability of corrosion in concrete structures.

1. Introduction

Corrosion of the steel reinforcement in concrete is a crucial problem for the construction industry since it poses the most serious risk to the structural integrity of reinforced concrete structures. Inspection and monitoring techniques are needed to assess the corrosion of the reinforcement in order to maintain, protect, and repair buildings and bridge decks so that they remain safe [1, 2]. In the last few years much attention has been given to developing techniques for predicting the remaining service life of concrete structures [3]. Most of the reported research in this area focuses on the corrosion of concrete reinforcement [4].

Several electrochemical techniques for monitoring and assessing the corrosion of steel in concrete structures were presented in [5–7]. The most popular method of *in situ* corrosion testing is the half-cell potential measurement, the idea of which is illustrated in Figure 1(a). The use of this method and the interpretation of its results are described in ASTM C876 [8]. Such corrosion potential measurements,

however, should be supplemented with other nondestructive testing methods [9–12]. The use of half-cell potential measurements for determining the probability of corrosion in concrete was extensively described by Flis et al. [13], Grantham et al. [14], and Žvica [15]. The latter also presented dependences between the rate of reinforcement corrosion and temperature. The effectiveness of the test was studied in [16]. It should be noted that half-cell potential values merely provide information about the probability of corrosion and not about the rate of corrosion.

It is well known that the probability of corrosion in concrete structures depends on the ionic conductivity of the concrete electrolyte, the humidity, the temperature, and the quality of the concrete cover. The ionic conductivity is measured quantitatively as the resistivity of the concrete [17]. Concrete resistivity ρ ranges widely from 10^1 to 10^6 Ω m, depending on mainly the moisture content [18] and the material of the concrete [19, 20]. One of the promising techniques of measuring concrete resistivity is shown in Figure 1(b). As shown by Feliiu et al. [21], concrete resistivity

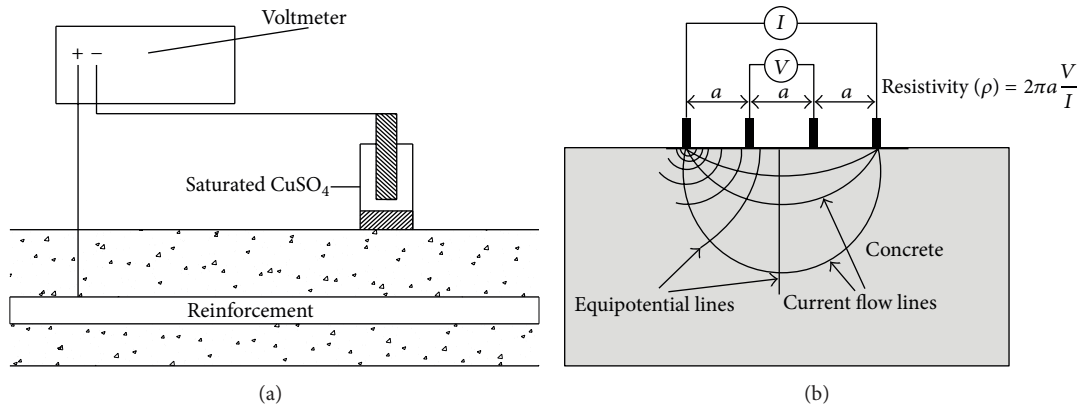


FIGURE 1: Existing corrosion methods: (a) half-cell potential measurement [27] and (b) concrete resistivity measurement [28].

TABLE 1: Dependence between potential and corrosion probability [8].

Potential E_{corr}	Probability of corrosion
$E_{\text{corr}} < -350 \text{ mV}$	Greater than 90% probability that reinforcing steel corrosion is occurring in that area at the time of measurement
$-350 \text{ mV} \leq E_{\text{corr}} \leq -200 \text{ mV}$	Corrosion activity of the reinforcing steel in that area is uncertain
$E_{\text{corr}} > -200 \text{ mV}$	90% probability that no reinforcing steel corrosion is occurring in that area at the time of measurement (10% risk of corrosion)

TABLE 2: Dependence between concrete resistivity and corrosion probability [34].

Concrete resistivity ρ , k Ω cm	Probability of corrosion
$\rho < 5$	Very high
$5 < \rho < 10$	High
$10 < \rho < 20$	Low to moderate
$\rho > 20$	Low

ρ is inversely proportional to the corrosion rate. This was confirmed by Glass et al. [22] who showed that the effect of mortar resistivity is strongly dependent on the relative humidity of the environment, while López et al. [23] showed that the amount of pores in concrete determines its resistivity ρ and corrosion rate. The four-point resistivity method enables one to determine the severity of corrosion in a quick and nondestructive manner. Morris et al. [24] found that rebars undergo active corrosion when concrete resistivity ρ is below 10 k Ω cm, whereas at concrete resistivity ρ above 30 k Ω cm the probability of their corrosion is low. Extensive research on the resistivity technique, covering experimental analyses [25] and an analysis of the effects of geometry and material properties [26], was done by Zhang et al.

It should be noted that in the literature there are only a few papers in which the probability of corrosion is determined using both concrete resistivity measurements and half-cell potential mapping. One of them is the paper by Millard and Sadowski [29] in which in order to determine the degree of corrosion of the reinforcement, the resistivity of the concrete is measured by the electrodes used in the half-cell potential method. The combined use of half-cell

potential and resistivity measurements was presented in [27]. In [28] it was shown that the combination of the method described in [29] and the conventional method of measuring concrete resistivity could be a reliable tool for directly determining the corrosion rate of the reinforcement in concrete. In paper [30] for this purpose Vedalakshmi et al. used the galvanostatic pulse technique with electrochemical impedance spectroscopy and the weight-loss method. Rhazi [31] measured concrete resistivity ρ in the same locations where half-cell potentials were measured, but it should be noted that the measurements were carried out on a concrete bridge deck covered with asphalt.

Considering that in the literature it is hard to find a systematic methodology for assessing the probability of corrosion in concrete slabs through combined half-cell potential and concrete resistivity measurements, this paper proposes such a methodology based on the combined use of the four-point Wenner concrete resistivity method and the half-cell potential method.

2. Methodology for Assessing Probability of Corrosion in Concrete Slabs

The proposed methodology for assessing the probability of corrosion in concrete slabs through a combination of two methods, that is, the half-cell potential method and the concrete resistivity method, is illustrated graphically in Figure 2.

Before measurements, the surface of the concrete slab should be prepared by brushing and polishing with abrasive paper, and a grid of n measuring points spaced at every 75 mm should be marked on the slab surface. Then the

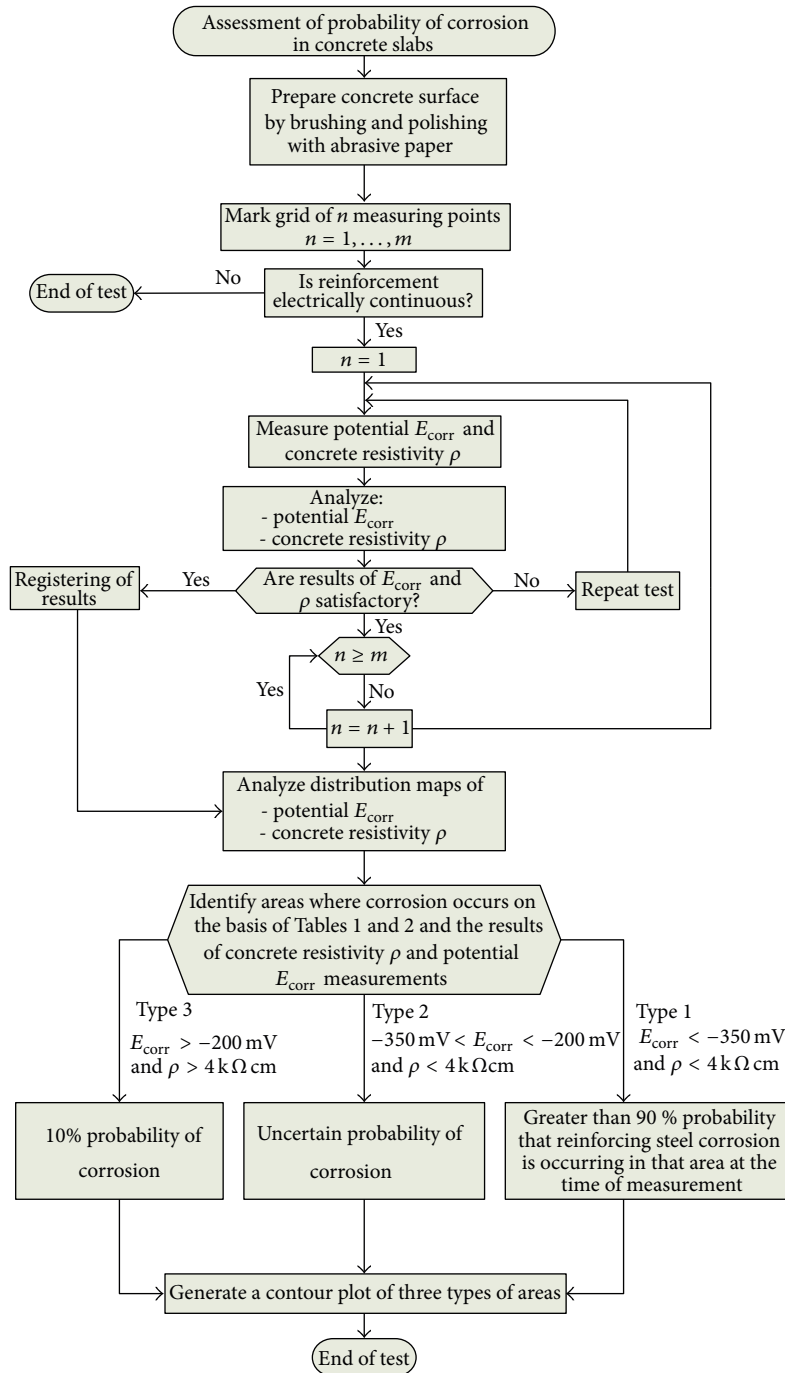


FIGURE 2: Assessment of probability of corrosion in concrete slabs through half-cell potential and concrete resistivity measurements.

electrical continuity of the reinforcement is checked in three randomly selected grid points. Subsequently potential E_{corr} and concrete resistivity ρ are measured. If the results of the E_{corr} and ρ measurements are satisfactory, they are processed using the specialized software and maps of the distribution of the parameter values on the slab surface are produced. The distribution maps of potential E_{corr} and concrete resistivity ρ should be examined. Table 2 summarizes the typical interpretation of half-cell potential readings [8]. The dependences between reinforcement corrosion probability and concrete

resistivity measured by the four-point Wenner method are shown in accordance with [32] in Table 3. If there is a probability of corrosion, one should identify the areas in which corrosion may occur. On the basis of Tables 1 and 2 and the results of the concrete resistivity ρ and potential E_{corr} measurements, three areas of different types can be generated:

- (i) area type 1—low values of both parameters, greater than 90% probability that reinforcing steel corrosion is occurring in that area at the time of measurement;

TABLE 3: Potential E_{corr} .

Nr	Potential E_{corr} , mV								
	A	B	C	D	E	F	G	H	I
1	-192	-168	-154	-151	-144	-156	-178	-192	-288
2	-240	-167	-169	-167	-168	-187	-201	-216	-276
3	-234	-168	-198	-189	-178	-189	-200	-215	-281
4	-201	-178	-201	-190	-189	-191	-200	-199	-291
5	-168	-165	-181	-191	-192	-189	-194	-192	-360
6	-231	-174	-182	-204	-201	-199	-194	-198	-365
7	-203	-164	-198	-219	-232	-231	-199	-196	-369
8	-216	-167	-197	-207	-216	-245	-234	-192	-384
9	-192	-168	-201	-231	-240	-245	-219	-216	-432

TABLE 4: Concrete resistivity ρ .

Nr	Concrete resistivity ρ , k Ω cm								
	A	B	C	D	E	F	G	H	I
1	6.91	5.62	4.56	4.56	4.34	4.12	4.08	4.39	3.77
2	9.11	5.96	4.63	4.57	4.56	4.34	4.23	4.38	3.76
3	9.89	5.98	4.85	4.78	4.67	4.22	5.03	5.02	3.75
4	9.88	5.99	5.99	4.23	4.78	4.89	5.65	5.33	3.71
5	9.99	6.02	6.98	4.8	4.76	5.02	5.43	5.35	3.74
6	9.45	6.25	6.71	5.43	4.23	5.03	5.68	5.67	3.67
7	9.77	6.66	6.77	5.55	7.51	5.42	5.43	5.21	3.62
8	9.73	6.71	6.88	6.01	7.01	5.98	5.67	4.88	3.61
9	8.79	6.91	6.93	6.96	6.98	6.91	5.96	4.71	3.14

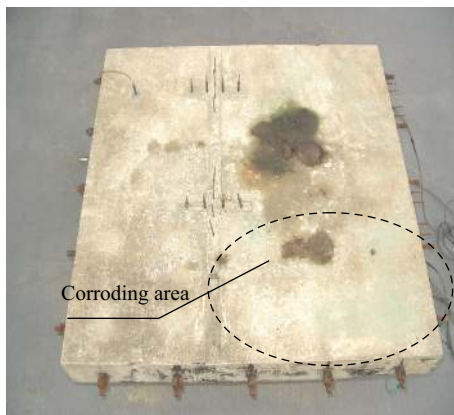


FIGURE 3: General view of concrete slab specimen.

- (ii) area type 2—low values of concrete resistivity ρ and high values of measured potential E_{corr} , an uncertain probability of corrosion;
- (iii) area type 3—high values of both parameters, a 10% probability of corrosion.

Finally, a contour plot of three types of areas (type 1, type 2, and type 3) should be generated.

The corrosion probability assessment can be practically verified through test pits made in selected places and visual inspection [33].

3. Exemplary Application of the Proposed Methodology

3.1. Materials and Methods. An exemplary application of the proposed methodology is presented below. 200 mm thick 750 mm \times 750 mm concrete slab specimen was investigated (Figure 3). The concrete had been designed to strengthen class C 20/25. Portland cement CEM I 42.5R, well-graded sand, and crushed blue granite with a maximum total grading of 5 mm, consistency S3, and $w/c = 0.5$ had been used to cast the slab specimens. A reinforcement mesh made of A-III 34GS steel rebars 10 mm in diameter spaced at every 150 mm with a 50 mm cover had been embedded inside each slab. The concrete slab specimen was placed in a normal atmosphere and was subjected to a two-hour spray wetting with a sodium chloride solution cycle followed by twenty hours drying cycle to generate corroding area presented in Figure 3.

Measurements were carried out after 90 days of concrete curing, except for compressive strength tests which were done after 28 days. The concrete slabs cured at an air temperature of $+18^{\circ}\text{C} (\pm 3^{\circ}\text{C})$ and a relative air humidity of 60%. It is important to measure concrete resistivity in constant temperature-humidity conditions since, as shown in [34], with each degree Celsius relative humidity increases by 3% [35]. After the concrete slabs were labelled, a 750 mm \times 750 mm test area was demarcated on each of them and a grid of points spaced at every 75 mm was marked on each of the slabs. The columns were denoted with letters from A to I, and



FIGURE 4: Half-cell potential measurements: (a) copper/copper sulphate electrode and (b) digital voltmeter.



FIGURE 5: Concrete resistivity measurement: (a) test setup and (b) measurement.

the rows were numbered from 1 to 9. A total of 81 measuring points were marked on the surface.

Prior to half-cell potential measurements, the electrical continuity of the reinforcement was checked at three randomly selected grid points. The potential differences in the three points were measured with a digital voltmeter, and all the measured values were found to be below 1 mV. The copper/copper sulphate electrode used in this test is shown in Figure 4(a), and the digital voltmeter with high input impedance is shown in Figure 4(b). Before the measurements, the concrete surface was prepared by brushing and polishing with abrasive paper. The area where each measurement was to be taken was wetted with tap water to ensure better electrical contact. Then the reference electrode and the reinforcement mesh were connected to the high-impedance voltmeter, and the reference electrode was placed on the surface of the concrete.

The concrete resistivity measurements were carried out at frequencies in a range of 50–1000 Hz. Before the measurements, the equipment was calibrated using a 1 k Ω calibration bar. A single deviation was not larger than 2% and the average deviation amounted to less than 1%. Concrete resistivity ρ was measured in each point of the grid (Figure 5).

3.2. Results

3.2.1. Half-Cell Potential Measurements. Exemplary results of the half-cell potential measurements are shown in Table 3. The results of the half-cell potential measurements were plotted on a contour map for visual interpretation (Figure 6). It is evident that potential E_{corr} is low (< -350 mV) in the area around measuring points 7 to 9 from E to I, which indicates a 95% probability of corrosion. In the other measuring points, potential E_{corr} is high (-350 mV $\leq E_{\text{corr}} \leq -200$ mV), which indicates a 10% or uncertain probability of corrosion.

3.2.2. Concrete Resistivity Measurements. The results of the concrete resistivity measurements are shown in Table 4. The results of the concrete resistivity measurements were plotted on an equipotential contour map for visual interpretation (Figure 7). It is evident that concrete resistivity ρ is low (< 5 k Ω cm) in the area around measuring points 5 to 9 from A to I, which indicates a very high probability of corrosion. In the other measuring points, concrete resistivity ρ is high (> 5 k Ω cm), indicating a high or moderate probability of corrosion.

3.3. Statistical Analyses of Test Results. Selected statistical characteristics of the parameters determined by half-cell

TABLE 5: Selected statistical characteristics of parameters determined by half-cell potential and concrete resistivity measurements.

	Statistical characteristics			
	Average	Standard deviation	Minimum	Maximum
Potential E_{corr} , mV	-211.09	53.46	-432	-144
Concrete resistivity ρ , k Ω cm	5.68	1.66	3.14	9.99

TABLE 6: Proposed types of corrosion probability.

		Potential E_{corr} , mV		
		$E_{corr} < -350$	$-350 \leq E_{corr} \leq -200$	$-200 \leq E_{corr}$
Concrete resistivity ρ , k Ω cm	$\rho < 4$	Type 1	Type 2	Type 2
	$4 < \rho < 5$			Type 3
	$\rho > 5$			Type 3

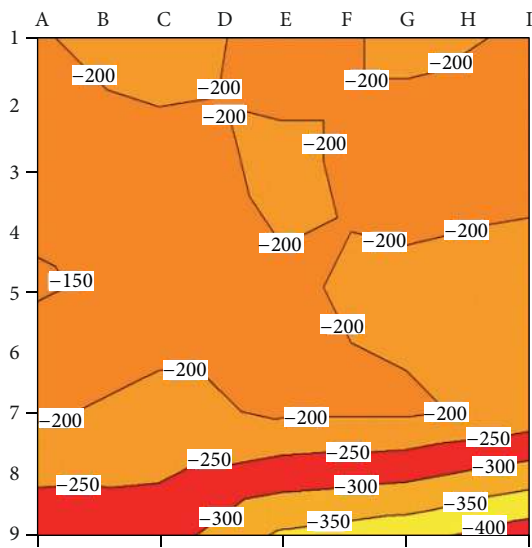


FIGURE 6: Contour plot of potential E_{corr} .

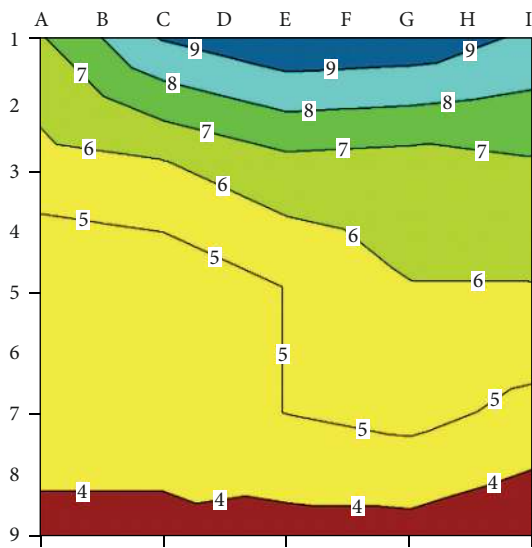


FIGURE 7: Contour plot of concrete resistivity ρ .

potential and concrete resistivity measurements are shown in Table 5. As it appears from the histograms presented in Figure 8 and statistical characteristics shown in Table 5, the half-cell potential method yielded potential E_{corr} ranging from -432 to -144 mV. The average value of potential E_{corr} was -211.09 mV with standard deviation of 53.46 mV.

Concrete resistivity ρ determined by concrete resistivity measurements ranged from 3.14 to 9.99 k Ω cm. The average value of concrete resistivity ρ was 5.68 k Ω cm with standard deviation of 1.66 k Ω cm.

3.4. Discussion. The dependence between concrete resistivity ρ and potential E_{corr} , measured on the concrete slab surface, is shown in Figure 9. One should note that potential E_{corr} sharply increases for resistivity ρ below 4 k Ω cm while above 4 k Ω cm, it oscillates between -150 and -250 mV.

On the basis of Tables 1 and 2 and the results of the concrete resistivity ρ and potential E_{corr} measurements, three areas of different types were generated (Table 6) as it has been presented in Section 2. A contourplot of the three areas is

shown in Figure 10. The area around measuring points 6 to 9 from C to I is of type 1, which means that there is a 90% probability of corrosion. In the measuring points, potential E_{corr} is below -250 mV and concrete resistivity ρ is above 4 k Ω cm. The area around measuring points 3 to 9 from A to E is of type 2, which means that there is a uncertain probability of corrosion. In the measuring points, potential E_{corr} is between -150 mV and -350 mV and concrete resistivity ρ is above 4 k Ω cm. The area around measuring points 1 to 7 from A to I is of type 3, which means that there is an 10% probability of corrosion. In the measuring points, potential E_{corr} is above -250 mV and concrete resistivity ρ is above 5 k Ω cm.

4. Conclusion

A methodology for assessing the probability of corrosion in concrete slabs based on a combination of two nondestructive methods, that is, the half-cell potential method and the concrete resistivity method, was briefly described. Comparative tests were carried out using the two methods to determine the probability of corrosion in model test concrete

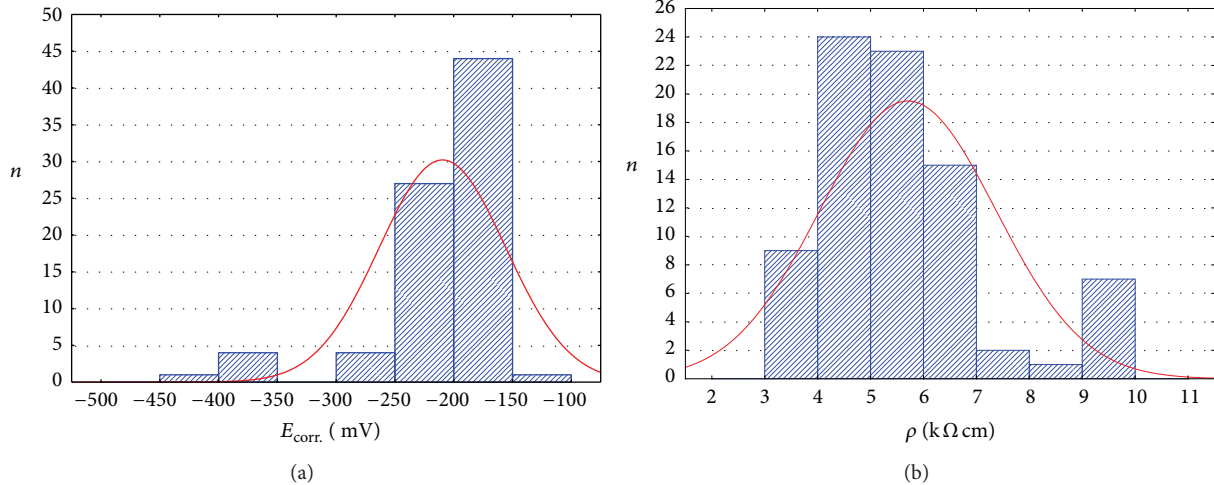


FIGURE 8: Histogram of (a) potential E_{corr} and (b) concrete resistivity ρ .

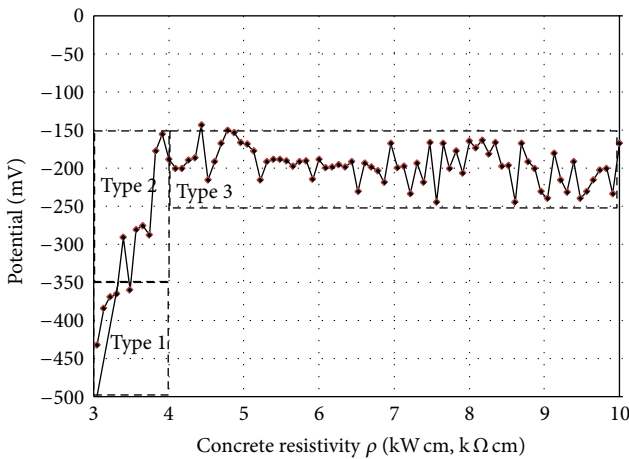


FIGURE 9: Concrete resistivity ρ versus potential E_{corr} .

slab specimens. The experimental results showed that the two nondestructive techniques can be used together in order to obtain maximum information about the probability of corrosion in a tested structure.

This study was motivated by the engineer’s need for a combination of the half-cell potential mapping technique and concrete resistivity measurements to more accurately assess the probability of corrosion. The combined techniques can be used in both the field and the laboratory environment. Moreover, they can be automated and integrated into monitoring systems for new or existing reinforced concrete structures. However, it is still recommended to perform additional tests for other rebar diameters, different aggregate grading, and a wider range of covers.

Acknowledgments

This research was carried out in collaboration with the Construction and Infrastructure Group in the University of

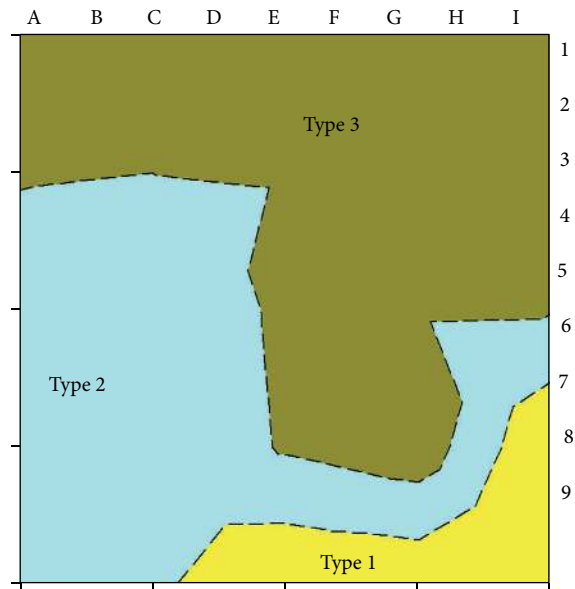


FIGURE 10: A contour plot of three areas of different types.

Liverpool under the project “Modern Nondestructive Testing Methods to Determine the Corrosion Rate in Concrete Structures” funded by the Erasmus LLP Programme.

References

- [1] J. Berger, S. Bruschetini-Ambro, and J. Kollegger, “An innovative design concept for improving the durability of concrete bridges,” *Structural Concrete*, vol. 12, no. 3, pp. 155–163, 2011.
- [2] M. Beck, A. Burkert, J. Harnisch et al., “Deterioration model and input parameters for reinforcement corrosion,” *Structural Concrete*, vol. 13, no. 3, pp. 145–155, 2012.
- [3] A. Lowinska-Kluge and T. Blaszczyński, “The influence of internal corrosion on the durability of concrete,” *Archives of Civil and Mechanical Engineering*, vol. 12, no. 2, pp. 219–227, 2012.

- [4] K. Ostermiski and P. Schießl, "Design model for reinforcement corrosion," *Structural Concrete*, vol. 13, no. 3, pp. 156–165, 2012.
- [5] H. Song and V. Saraswalhy, "Corrosion monitoring of reinforced concrete structures—a review," *International Journal of Electrochemical Science*, vol. 2, pp. 1–28, 2007.
- [6] C. Andrade, C. Alonso, J. Gulikers et al., "Test methods for on-site corrosion rate measurement of steel reinforcement in concrete by means of the polarization resistance method," *Materials and Structures*, vol. 37, no. 273, pp. 623–643, 2004.
- [7] G. Sposito, P. Cawley, and P. B. Nagy, "Potential drop mapping for the monitoring of corrosion or erosion," *NDT and E International*, vol. 43, no. 5, pp. 394–402, 2010.
- [8] "ASTM C876-91: standard test method for half-cell potentials of uncoated reinforcing steel in concrete," 1999.
- [9] J. Hoła and M. Ksiazek, "Research on usability of sulphur polymer composite for corrosion protection of reinforcing steel in concrete," *Archives of Civil and Mechanical Engineering*, vol. 9, no. 1, pp. 47–59, 2009.
- [10] M. Kosior-Kazberuk and W. Jezierski, "Evaluation of concrete resistance to chloride ions penetration by means of electric resistivity monitoring," *Journal of Civil Engineering and Management*, vol. 11, no. 2, pp. 109–114, 2005.
- [11] J. Hoła and K. Schabowicz, "State-of-the-art non-destructive methods for diagnostic testing of building structures—anticipated development trends," *Archives of Civil and Mechanical Engineering*, vol. 10, no. 3, pp. 5–18, 2010.
- [12] K. Liam, S. Roy, and D. Northwood, "Chloride ingress measurements and corrosion potential mapping study of a 24-year-old reinforced concrete jetty structure in a tropical marine environment research," *Magazine of Concrete Research*, vol. 44, pp. 205–215, 1992.
- [13] J. Flis, H. W. Pickering, and K. Osseo-Asare, "Assessment of data from three electrochemical instruments for evaluation of reinforcement corrosion rates in concrete bridge components," *Corrosion*, vol. 51, no. 8, pp. 602–609, 1995.
- [14] M. G. Grantham, B. Herts, and J. Broomfield, "The use of linear polarisation corrosion rate measurements in aiding rehabilitation options for the deck slabs of a reinforced concrete underground car park," *Construction and Building Materials*, vol. 11, no. 4, pp. 215–224, 1997.
- [15] V. Žvica, "Possibility of improvement of potentiodynamic method for monitoring corrosion rate of steel reinforcement in concrete," *Bulletin of Materials Science*, vol. 24, no. 5, pp. 555–558, 2001.
- [16] S. Erdogdu, I. L. Kondratova, and T. W. Bremner, "Determination of chloride diffusion coefficient of concrete using open-circuit potential measurements," *Cement and Concrete Research*, vol. 34, no. 4, pp. 603–609, 2004.
- [17] N. Bowler and Y. Huang, "Electrical conductivity measurement of metal plates using broadband eddy-current and four-point methods," *Measurement Science and Technology*, vol. 16, no. 11, pp. 2193–2200, 2005.
- [18] T. Gorzelańczyk, "Moisture influence on the failure of self-compacting concrete under compression," *Archives of Civil and Mechanical Engineering*, vol. 11, no. 1, pp. 45–60, 2011.
- [19] R. Polder, C. Andrade, B. Elsener et al., "Test methods for on site measurement of resistivity of concrete," *Materials and Structures*, vol. 33, pp. 603–611, 2000.
- [20] B. Elsener, L. Bertolini, P. Pedferri, and R. Polder, *Corrosion of Steel in Concrete—Prevention, Diagnosis, Repair*, Wiley-Vch, Berlin, Germany, 2004.
- [21] S. Feliu, J. A. Gonzalez, S. Feliu, and M. C. Andrade, "Confinement of the electrical signal for in situ measurement of polarization resistance in reinforced concrete," *ACI Materials Journal*, vol. 87, no. 5, pp. 457–460, 1990.
- [22] G. K. Glass, C. L. Page, and N. R. Short, "Factors affecting the corrosion rate of steel in carbonated mortars," *Corrosion Science*, vol. 32, no. 12, pp. 1283–1294, 1991.
- [23] W. López, J. A. González, and C. Andrade, "Influence of temperature on the service life of rebars," *Cement and Concrete Research*, vol. 23, no. 5, pp. 1130–1140, 1993.
- [24] W. Morris, A. Vico, M. Vazquez, and S. R. de Sanchez, "Corrosion of reinforcing steel evaluated by means of concrete resistivity measurements," *Corrosion Science*, vol. 44, no. 1, pp. 81–99, 2002.
- [25] J. Zhang, P. J. M. Monteiro, and H. F. Morrison, "Noninvasive surface measurement of corrosion impedance of reinforcing bar in concrete—part 1: experimental results," *ACI Materials Journal*, vol. 98, no. 2, pp. 116–125, 2001.
- [26] J. Zhang, P. J. M. Monteiro, H. F. Morrison, and M. Mancio, "Noninvasive surface measurement of corrosion impedance of reinforcing bar in concrete—part 3: effect of geometry and material properties," *ACI Materials Journal*, vol. 101, no. 4, pp. 273–280, 2004.
- [27] B. Elsener, C. Andrade, J. Gulikers, R. Polder, and M. Raupach, "Half-cell potential measurements—potential mapping on reinforced concrete structures," *Materials and Structures*, vol. 36, no. 261, pp. 461–471, 2003.
- [28] L. Sadowski, "New non-destructive method for linear polarisation resistance corrosion rate measurement," *Archives of Civil and Mechanical Engineering*, vol. 10, no. 2, pp. 109–116, 2010.
- [29] S. Millard and L. Sadowski, "Novel method for linear polarisation resistance corrosion measurement," *e-Journal of Nondestructive Testing & Ultrasonics*, vol. 14, 2009.
- [30] R. Vedalakshmi, L. Balamurugan, V. Saraswathy, S. H. Kim, and K. Y. Ann, "Reliability of Galvanostatic Pulse Technique in assessing the corrosion rate of rebar in concrete structures: laboratory vs field studies," *KSCE Journal of Civil Engineering*, vol. 14, no. 6, pp. 867–877, 2010.
- [31] J. Rhazi, "Test method for evaluating asphalt-covered concrete bridge decks using ground penetrating radar," in *PIERS Proceedings*, Marrakesh, Morocco, 2011.
- [32] J. Bungey and S. Millard, *Testing of Concrete in Structures*, Chapman & Hall, Glasgow, UK, 1996.
- [33] E. Bardal and J. Drugli, "Corrosion detection and diagnosis," in *Materials Science and Engineering, Vol. 3, Encyclopedia of Life Support Systems*, R. D. Rawlings, Ed., 2004.
- [34] W. Elkey and E. Sellevold, *Electrical Resistivity of Concrete*, Publication no. 80, Norwegian Road Research Laboratory, Oslo, Norway, 1995.
- [35] L. Sadowski, "Non-destructive investigation of corrosion current density in steel reinforced concrete by artificial neural networks," *Archives of Civil and Mechanical Engineering*, vol. 13, no. 1, pp. 104–111, 2013.



Hindawi

Submit your manuscripts at
<http://www.hindawi.com>

